SPIE 3rd International Asia Pacific Environmental Remote Sensing Symposium, 23-27 October 2002, Hangzhou, China.
To appear in: Ocean Remote Sensing and Applications, SPIE Proc. Vol. 4892.

Mapping optical parameters of coastal sea waters using the Hyperion imaging spectrometer

Soo Chin Liew* and Leong Keong Kwoh

Centre for Remote Imaging, Sensing and Processing
National University of Singapore

ABSTRACT

The Hyperion instrument on-board the EO1 satellite is an imaging spectrometer capable of acquiring hyperspectral data with over 200 contiguous spectral bands of about 10 nm bandwidth. The instrument is not designed for ocean observation. Nevertheless, case 2 water near the coastal regions with high sediment loading usually has higher reflectance in the visible wavelength region than the clear case 1 water in the open oceans. Hence, the signal-to-noise ratio of Hyperion data over coastal waters may be sufficiently high, such that meaningful measurements of the optical properties of the coastal sea waters are possible. We tested the use of Hyperion imagery in retrieving and mapping the distributions of the coastal sea water optical parameters in the Singapore Strait. The Hyperion reflectance spectra were fitted to a coupled sea water reflectance and atmospheric transmission model. The water reflectance corrected for atmospheric effects could be computed from the fitting parameters. This method of inverse modeling by spectral fitting was able to separate the confounding effects due to scattering by suspended sediments and absorption by chlorophyll and dissolved organic matter. Spatial distributions of these three main constituents of coastal waters could be obtained.

Keywords: coastal waters, optical parameters, scattering, absorption, hyperspectral imaging, reflectance, sediments, dissolved organic matter, chlorophyll

1. INTRODUCTION

Satellite remote sensing provides an important tool for large-scale monitoring of the coastal environment. Currently, several space-borne ocean color instruments are available for assessment of the marine productivity, phytoplankton biomass, suspended sediment load and other parameters. These sensors (e.g. CZCS, OCTS, SeaWiFS, and MODIS) are designed primarily for observing the global oceans, with a typical spatial resolution of 1 km. Due to the interference of stray lights from land, the region of coastal waters a few km from the coast is usually masked out before the data are being processed. Higher resolution instruments are needed in the observation of coastal waters. High resolution satellite sensors such as LANDSAT and SPOT are optimized for land applications and do not have the spectral specificity for quantitative study of the coastal waters. The recently launched MERIS instrument on board the ENVISAT satellite is similar to MODIS in spectral bands and resolution, but it has a fine resolution mode of 300-m, and thus is more suitable for coastal zone applications. The NASA's EO-1 satellite (launched in November 2000) carries on board the Hyperion instrument, which is a high spatial resolution (30 m) hyperspectral imaging instrument. Hyperion has over 200 contiguous spectral bands, each with a bandwidth of 10 nm, spanning the wavelength region from the visible-near infrared (VNIR) to the short-wave infrared (SWIR) regions. This instrument is designed primarily for land applications and the signal-to-noise ratio is often thought to be sub-optimal for ocean applications. Nevertheless, case 2 coastal waters with a high sediment load usually have a higher reflectance in the visible wavelength region than the clear case 1 waters in the open oceans. Hence, the signal-to-noise ratio of Hyperion data over coastal waters may be sufficiently high, such that meaningful measurements of the optical properties of the coastal sea waters may be possible.

* Corresponding author; email scliew@nus.edu.sg; phone (+65) 68745069; fax (+65) 67757717; http://www.crisp.nus.edu.sg; Centre for Remote Imaging, Sensing and Processing, National University of Singapore, Blk. SOC-1 Level 2, Lower Kent Ridge Road, Singapore 119260, Republic of Singapore.

Coastal waters are typically cast 2 waters. Unlike the case 1 waters of the open ocean, the optical properties of case 2 waters are not influenced by chlorophyll alone. The presence of dissolved organic matters and suspended sediments not covarying with chlorophyll complicates the task of retrieving the optical properties from reflectance. The optical properties of the sea waters are usually modeled by the three component model[1], where the absorption and scattering coefficients of water are determined by the concentrations of the gelbstof or colored dissolved organic matter (CDOM), phytoplankton and non-chlorophyllous particles. The conventional algorithms for the retrieval of the sea water constituents such as chlorophyll are usually based on the ratio of radiance or reflectance measured in the blue and green spectral bands[2]. The chlorophyll concentration is found by applying a polynomial derived from regression of the band ratio with the sea-truth values of chlorophyll concentration measured at various places. This method works well in open ocean waters (case 1 waters)[3], but is generally found to be inadequate for case 2 waters[4].

In this paper, we present our findings on the use of the Hyperion imagery in mapping the optical parameters of coastal sea waters in a coastal region near Singapore. We use an inverse modeling technique[5, 6, 7] to retrieve the optical parameters of the coastal sea water from Hyperion data. Both the optical properties of the sea water and the atmosphere are modeled. Essentially, the reflectance spectrum measured by the sensor over the sea water is fitted to a coupled sea water reflectance and atmospheric transmission model. Given a set of parameters including the optical parameters of the various water constituents and the atmosphere, a reflectance spectrum is computed using the model. The measured reflectance spectrum is compared with this computed spectrum. The deviation between the computed and measured spectra is minimized by varying the input parameters to the model, with the help of an optimizing procedure. The set of parameters values that produces the minimum deviation is then taken as the retrieved parameters values.

2. HYPERION DATA SET

Hyperion data processed to Level 1A at the NASA Goddard Space Flight Center EO1 Data Processing Facility was used. The test area is located at the western part of the Singapore Strait, south of the main island of Singapore. The Hyperion data over the Singapore Strait was acquired on day 153 of the year 2001. Only the visible and near infrared (VNIR) bands of the Hyperion data set were used in the study. The first few bands of the visible bands were rather noisy and were discarded. The wavelength bands used ranged from 447.9 nm (band 10) to 905.5 nm (band 55). The digital numbers were first calibrated to radiance values and then converted to top-of-atmosphere (TOA) reflectance. In order to improve the signal-to-noise ratio, an averaging low-pass filter (10 x 10 window size) was applied to each band of the data cube. The original resolution of the Hyperion data was 30 m. So this filtering process effectively degraded the resolution to 300 m. The data cube was then resampled to a pixel size of 150 m. A land mask was constructed by simply thresholding the normalized difference vegetation index (NDVI) constructed from the 804 nm and 672 nm bands. All pixels with zero or positive NDVI values were considered to be land pixels and were excluded from further processing.

3. METHODS

The TOA reflectance $R(\lambda)$ is fitted to the model for water reflectance and atmospheric transmission given by the following equation,

$$R(\lambda) = T_r T_a \left[T_w R_w(\lambda) + R_F(\lambda) + r \right] + R_r(\lambda) + R_a(\lambda) \tag{1}$$

The product $T_r T_a$ is the two-way atmospheric transmission due to Rayleigh and aerosol scattering while $R_r(\lambda)$ and $R_a(\lambda)$ are path radiance due to the two components. The Rayleigh scattering component can be computed analytically[8] while the transmission and path reflectance of the aerosol scattering component are modeled assuming an inverse power law with respect to the wavelength for the aerosol optical thickness. The reflectance of water just below the water surface is modeled by

$$R_w(\lambda) = K \frac{b_b(\lambda)}{a(\lambda) + b_b(\lambda)} \tag{2}$$

where $a(\lambda)$ and $b_b(\lambda)$ are the absorption and backscattering coefficients of the sea water and the parameter K takes the value 0.33. The contribution due to chlorophyll fluorescence is modeled by the term $R_F(\lambda)$ which takes the form of a

Gaussian function[9] peaked at 685 nm with a full-width at half-maximum of 25 nm. The models for the absorption and backscattering functions have been described previously[7]. The main parameters in the absorption and backscattering terms are the chlorophyll absorption coefficient at 440 nm (P440), CDOM absorption coefficient at 440 nm (G440) and the suspended sediment backscattering coefficient at 550 nm (X550). The factor T_w in equation (1) is the two way transmission factor through the water-air interface, and is characterized by the effective surface reflectance r and the refractive index of water.

Each TOA reflectance spectrum in the Hyperion data cube is fitted to the model (1) by finding a set of the fitting parameters that best fits the reflectance curve to the model. The downhill simplex method[10] is used to find the optimized parameters in the curve fitting procedure. The routines in ref. 10 were modified to impose constraints on the minimum and maximum values for each of the parameters. No correction has been done for absorption due to water vapor and other atmospheric gases. Thus, the wavelength bands above 700 nm where absorption occurs are not used in computing the chi-squared value (i.e. the parameter to be minimized that determines the goodness of fit) when performing the fitting procedure.

4. RESULTS AND DISCUSSIONS

An RGB composite image of the test area composed from three bands (651nm, 550nm and 448nm) of the Hyperion data cube is shown in Fig. 1. Regions of different water colors and brightness can be seen in this image. The stretch of water between the Jurong Island and the Main Island has a low reflectance and appears dark in the image, compared to the brighter region towards the south. The reflectance spectra at four sampling points along a transect marked in the figure are also shown, together with the best-fit spectra. The different colors of the sea water at these sampling points are also reflected in the different magnitude and shape of the spectra. Fig. 2 shows the spatial distributions of the backscattering coefficient due to suspended sediments, absorption coefficients due to CDOM and chlorophyll obtained by spectral fitting method.

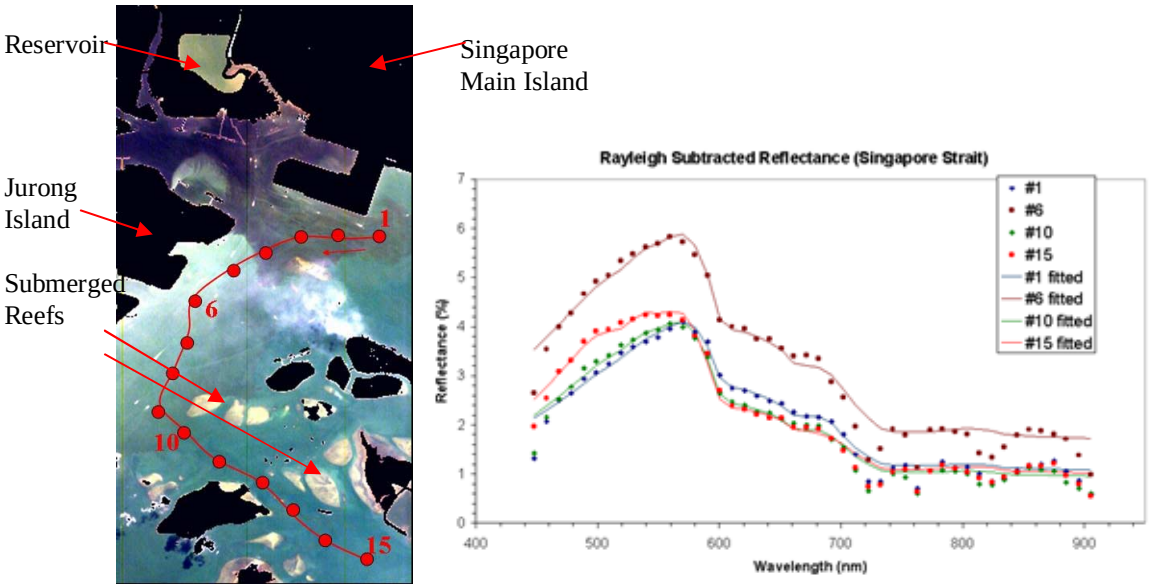

Fig. 1: True color composite of a Hyperion image of the Singapore Strait (red: 651 nm, green: 549.6 nm, blue: 447.9 nm). The land area has been masked out. The image is stretched to highlight regions of different water colors. The width of the image is about 7.5 km. The Rayleigh-subtracted reflectance spectra at the four sampling points (#1, #6, #10, #15) are shown on the right together with their respective fitted spectra.

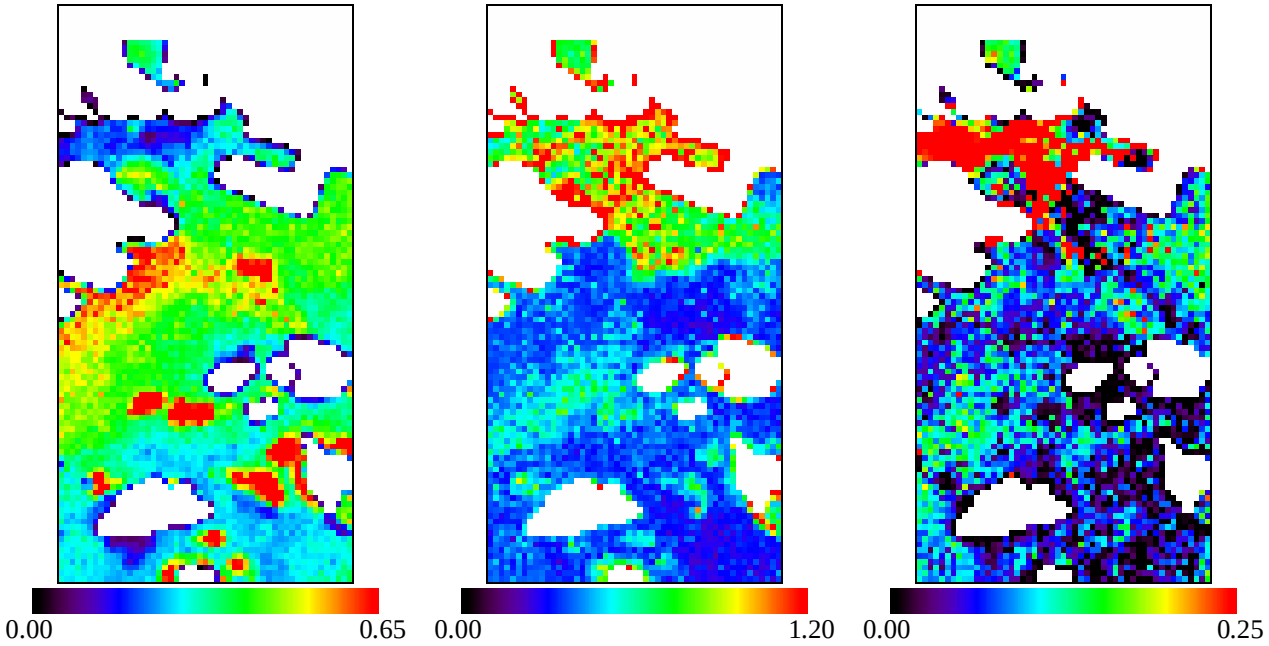

Fig. 2: Spatial distributions of the suspended sediment backscattering coefficient at 550 nm (left), CDOM absorption coefficient at 440 nm (middle) and chlorophyll absorption coefficient at 440 nm (right) in the test area. The color scale bars (with the min. and max. scale values in m^{-1}) are shown below the images.

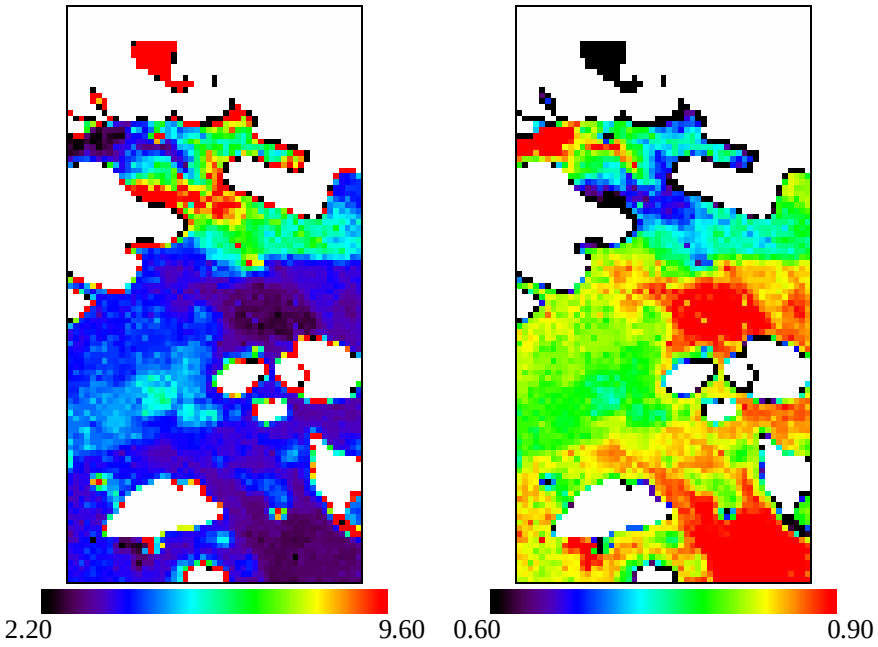

Fig. 3: Spatial distribution of the OC2 chlorophyll concentration (mg/m^3) (left) derived from the reflectance band ratio R489/R550 (right) using the SeaWiFS OC2 algorithm.

The sediment backscattering (Fig. 2, left) generally correlates with the brightness of the image in Fig. 1. The submerged reefs show up as regions of exceptionally high backscattering. Since the sea bottom effect is not included in the model, these regions are excluded from further analysis. The sharp boundary separating the dark region in the north and the bright region in the south (Fig. 1) is not present in the backscattering image. On the other hand, this boundary is clearly visible in the CDOM absorption image (Fig. 2, middle). It can thus be inferred that the dark water region is due to a high CDOM concentration, while the suspended sediment concentration does not differ much from the other areas. This is illustrated in the scatter plot of the sediment backscattering coefficient at 550 nm (X550) versus the reflectance at 550 nm (R550). The data points separate into two clusters, corresponding to the dark water area with a higher CDOM concentration and the brighter areas with a lower CDOM concentration.

The map of the spatial distribution of chlorophyll absorption (Fig. 2, right) is more noisy, but it seems to resemble the distribution of CDOM in the brighter water area. In fact, these two are moderately correlated (R^2=0.65), as shown in the scatter plot in Fig. 5. Chlorophyll absorption is expected to vary with the chlorophyll concentration in the sea water. Several simple algorithms for computing chlorophyll concentration are available. These algorithms are mainly based on the ratio of reflectance in the blue and green bands. The SeaWiFS OC2 chlorophyll algorithm employs the ratio of the 490 nm band reflectance to the 555 nm band reflectance. The chlorophyll concentration (Chl) value is computed according to the equation[2]:

$$\log_{10}(Chl - a_4) = a_0 + a_1 L + a_2 L^2 + a_3 L^3;\ \text{where}\ L = \log_{10}\left[\frac{R(490nm)}{R(555nm)}\right] \tag{3}$$

and the coefficients are

$$a_0 = 0.3410,\ a_1 = -0.3001,\ a_2 = 2.8110,\ a_3 = -2.0410\ \text{and}\ a_4 = -0.0400. \tag{4}$$

The Hyperion does not have a wavelength band centered at 555 nm, so the nearest band centered at 550 nm is used instead to compute the equivalent OC2 chlorophyll from the Hyperion data.

The OC2 chlorophyll computed from the band ratio R489/R550 correlates weakly with the chlorophyll absorption coefficient at 440 nm (R^2=0.29) when a power law relation is used to fit the band ratio to chlorophyll absorption (Fig. 6, left). This result is not surprising since the band ratio algorithm for computing chlorophyll is not expected to work well in case 2 waters where the water absorption in the blue band is influenced not only by chlorophyll, but also by the presence of CDOM. In cases where CDOM absorption is more dominant, the blue to green band ratio should be influenced more by CDOM, rather than chlorophyll. This is indeed the case. As shown in Fig. 6, the CDOM absorption exhibits a stronger correlation with the OC2 chlorophyll value (R^2=0.61).

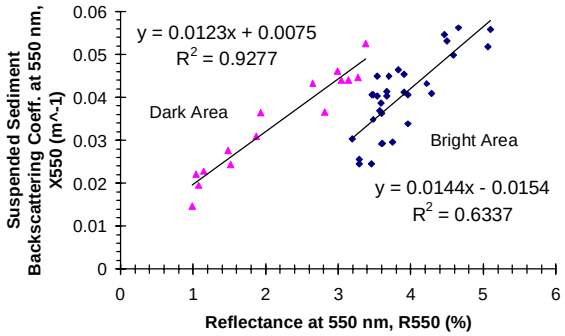

Fig. 4: Scatter plot of the suspended sediment backscattering coefficient at 550 nm versus the reflectance at 550 nm for the dark water area (triangles) and the brighter water area (diamonds). The submerged reef areas have been excluded in the plot.

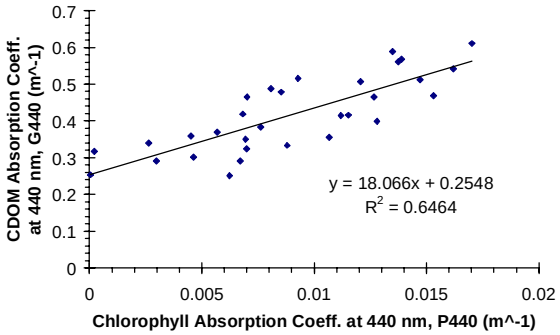

Fig. 5: Scatter plot of the CDOM absorption coefficient at 440 nm versus the chlorophyll absorption coefficient at 440 nm for the bright water area.

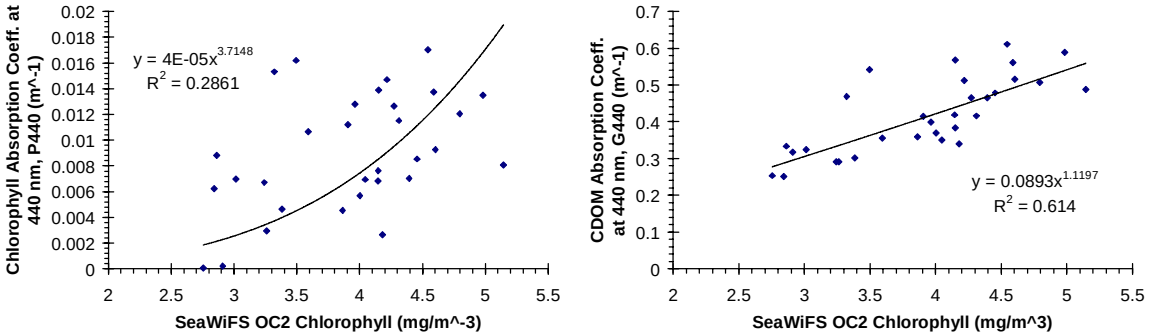

Fig. 6: Correlations of chlorophyll absorption coefficient at 440 nm (left) and CDOM absorption coefficient at 440 nm (right) with the chlorophyll concentration computed using the SeaWiFS OC2 algorithm.

5. CONCLUDING REMARKS

In this study, we have demonstrated the merit of the Hyperion imaging spectrometer in retrieving and mapping the optical parameters of turbid coastal waters. We have used a spectral fitting method of inverse modeling to retrieve the optical parameters. Unlike the conventional methods based on band ratios, the spectral fitting method makes use of the information contained in the full spectrum in the retrieval procedure. The band-ratio method works well in case 1 waters where the optical properties are influenced only by chlorophyll and co-varying constituents in the ocean. However, it often breaks down in case 2 waters where the blue bands absorption is influenced by both chlorophyll and CDOM. The band-ratio based algorithm is not able to separate the two components and thus often over-estimates the chlorophyll concentration in coastal waters. Comparison with the SeaWiFS OC2 algorithm derived chlorophyll values reveals that the OC2 chlorophyll has a higher correlation with CDOM absorption than chlorophyll absorption. As shown in Fig. 2 and Fig. 3, the spectral fitting method is able to deconvolute the effects of the three main water constituents, viz. suspended sediments, CDOM and chlorophyll such that the spatial distributions of these constituents can be mapped.

ACKNOWLEDGMENTS

The main author (S. C. Liew) is a member of the NASA's EO-1 science validation team (SVT). The assistance and support given by the EO-1 SVT, especially Dr. Stephen Ungar is greatly appreciated.

REFERENCES

1. S. Sathyendranath, L. Prieur, and A. Morel, "A three component model of ocean color and its application to remote sensing of phytoplankton pigments in coastal waters," *Int. J. Remote Sens.* **10**, pp. 1373-1394, 1989.
2. J. E. O'Reilly, S. Maritorena, B. G. Mitchell, D. A. Siegel, K. L. Carder, S. A. Garver, M. Kahru, and C. McClain, "Ocean color chlorophyll algorithms for SeaWiFS," *J. Geophys. Res.* **103C**, pp. 24937-24953, 1998.
3. A. Morel, "Optical properties of oceanic Case I waters, revisited," *Ocean Optics XIII*, SPIE Proc. **2963**, pp. 108-114, 1996.
4. S. Tassan, "Local algorithms using SeaWiFS data for the retrieval of phytoplankton, pigments, suspended sediment, and yellow substance in coastal waters," *Appl. Opt.* **33**, pp. 2369-2378, 1994.
5. R. Doerffer and J. Fischer, "Concentrations of chlorophyll, suspended matter, and gelbstoff in case II waters derived from satellite coastal zone color scanner data with inverse modeling methods," *J. Geophys. Res.* **99C**, pp. 7457-7466, 1994.
6. Z. Lee, K. L. Carder, C. D. Mobley, R. G. Steward, and J. S. Patch, "Hyperspectral remote sensing for shallow waters. II. Deriving bottom depths and water properties by optimization," *Appl. Optics* **38**, pp. 3831-3843, 1999.
7. S. C. Liew, A. S. Chia, K. H. Lim and L. K. Kwoh, “Modeling the reflectance spectra of tropical coastal waters,” *SPIE Proceedings* vol. 4488, pp. 248 - 255, 2001.
8. E. F. Vermote, D. Tanre, J. L. Deuzé, M. Herman, and J. J. Morcrette, “Second simulation of the satellite signal in the solar spectrum, 6S: An overview,”, *IEEE Trans. Geosc. Remote Sens.* 35, pp. 675-686, 1997.
9. J. F. R. Gower, R. Doerffer and G. A. Borstad, "Interpretation of the 685 nm peak in water-leaving radiance spectra in terms of fluorescence, absorption and scattering, and its observation by MERIS," Int. J. Rem. Sens. 20, pp. 1771-1786, 1999.
10. W. H. Press, S. A. Teukolsky, W. T. Vetterling, and B. P. Flannery, Numerical recipes in C: the art of scientific computing, 2nd ed., Cambridge U Press, Cambridge, 1992.